



**HAL**  
open science

## Study of the non-covalent coating of graphene-coated cobalt magnetic nanoparticles with pyrene-tagged dendritic poly(vinylidene fluoride)

Enrique Folgado, Marc Guerre, Nidhal Mimouni, Vincent Collière, Christian Bijani, Kathleen Moineau-Chane Ching, Anne-Marie Caminade, Vincent Ladmiral, Bruno Ameduri, Armelle Ouali

### ► To cite this version:

Enrique Folgado, Marc Guerre, Nidhal Mimouni, Vincent Collière, Christian Bijani, et al.. Study of the non-covalent coating of graphene-coated cobalt magnetic nanoparticles with pyrene-tagged dendritic poly(vinylidene fluoride). *ChemPlusChem*, 2019, 84 (1), pp.78-84. 10.1002/cplu.201800471 . hal-01996630

**HAL Id: hal-01996630**

**<https://hal.science/hal-01996630>**

Submitted on 30 Oct 2020

**HAL** is a multi-disciplinary open access archive for the deposit and dissemination of scientific research documents, whether they are published or not. The documents may come from teaching and research institutions in France or abroad, or from public or private research centers.

L'archive ouverte pluridisciplinaire **HAL**, est destinée au dépôt et à la diffusion de documents scientifiques de niveau recherche, publiés ou non, émanant des établissements d'enseignement et de recherche français ou étrangers, des laboratoires publics ou privés.

# $\pi$ -Stacking Interactions of Graphene-Coated Cobalt Magnetic Nanoparticles with Pyrene-Tagged Dendritic Poly(Vinylidene Fluoride)

Enrique Folgado,<sup>[a]</sup> Marc Guerre,<sup>[a]</sup> Nidhal Mimouni,<sup>[b,c]</sup> Vincent Collière,<sup>[b,c]</sup> Christian Bijani,<sup>[b,c]</sup> Kathleen Moineau-Chane Ching,<sup>[b,c]</sup> Anne-Marie Caminade,<sup>[b,c]</sup> Vincent Ladmiral,<sup>[a]</sup> Bruno Améduri<sup>[a]</sup> and Armelle Ouali<sup>\*[a]</sup>

**Abstract:** This study investigates the non-covalent coating of cobalt magnetic nanoparticles (MNPs) involving graphene surface with pyrene-tagged dendritic poly(vinylidene fluoride) (PVDF). Dendrimers bearing a pyrene moiety were selected to play the role of spacers between the graphene surface of the MNPs and the PVDF chains, the pyrene unit being expected to interact with the surface of the MNPs. The pyrene-tagged dendritic spacer **11** decorated with ten acetylenic functions was successfully prepared and fully characterized. Azido-functionalized PVDF chains were then grafted onto each branch of the dendrimer using Huisgen's [3+2] cycloadditions. Afterward, the association of the resulting pyrene-tagged dendritic PVDF **13** with commercially available Co/C MNPs by  $\pi$ -stacking interactions was studied by fluorescence spectroscopy. Besides, the stability of the  $\pi$ -stacking interactions when the temperature increases and the reversibility of the process upon the temperature decrease were also evaluated. Lastly, hybrid MNPs were prepared from pyrene-tagged dendrimers decorated either with acetylenic functions (**11**) or with PVDF branches (**13**), and they were characterized by transmission electron microscopy and comparative elemental analysis with naked MNPs.

## Introduction

Polymer-coated nanoparticles are of great interest for both industry and academic research laboratories for various applications in materials science or in biosciences.<sup>[1]</sup> Besides, nanoparticles (NPs) display a high surface-to-volume ratio creating large interfacial areas at the origin of unique properties compared to their micro- or macro-scale counterparts. Therefore, dispersing nanoparticles in polymer matrices allows the design of novel polymer nanocomposites materials that combine the properties and functions of both the NP and the polymer.<sup>[1]</sup>

However, this task is intrinsically difficult and challenging since attractions between NPs prevent their homogeneous dispersions. This is particularly true for magnetic nanoparticles (MNPs).<sup>[1]</sup>

The present work aims at studying the non-covalent coating of MNPs with dendritic<sup>[2]</sup> poly(vinylidene fluoride) (PVDF)<sup>[3,4]</sup> (Figure 1). PVDF is an interesting fluoropolymer with remarkable properties such as thermal stability, barrier properties, chemical inertness to solvents and acids as well as piezo-, pyro- and ferroelectric properties.<sup>[3]</sup> Targeting materials combining such advantages together with magnetic properties thus appears as a challenging and valuable objective. The hybrid MNPs targeted here may constitute key building blocks for the dispersion of MNPs in the PVDF matrix and lead to highly attractive nanocomposites. Such functional nanocomposites could find applications in the growing fields of printed and flexible electronics, binders for lithium ion batteries, and additives for coatings. The MNPs chosen as models are cobalt nanoparticles coated with graphene layers (Co/C MNPs).<sup>[5]</sup> First described by Grass et al.<sup>[5]</sup> and now commercially available,<sup>[6]</sup> these NPs are prepared by reducing flame synthesis while the core-shell arrangement is achieved by the addition of acetylene to the cobalt-nanoparticle-forming process, resulting in the controlled deposition of carbon sheet onto the particles. To date, these MNPs have been widely employed as supports for homogeneous catalysts or adsorbents and the main interest of the resulting magnetic constructs is their recovery by magnetic decantation and possible reuse.<sup>[7-12]</sup>

Interestingly, the graphene surface of the MNPs makes their functionalization possible using either covalent chemistry or by resorting to a non-covalent strategy. Only a few reports describe the grafting of pyrene-tagged functional species (e. g. boradiazaindacene fluorescent dye<sup>[8]</sup> or palladium catalyst<sup>[9]</sup>) onto the graphene surface of MNPs through  $\pi$ -stacking interactions.<sup>[7]</sup> The present work focuses on this by far less studied non-covalent strategy to coat MNPs with polymers. Although  $\pi$ -stacking interactions were used to graft pyrene-tagged polymers onto carbon nanotubes,<sup>[10]</sup> it has never been reported for the grafting of polymers onto the surface of such Co/C MNPs. Indeed, usual strategies mainly involve the covalent grafting to graphene surface via a phenyl or a biphenyl linker.<sup>[12]</sup>

Besides, whatever the grafting strategy used (either covalent or by  $\pi$ -stacking), only low density of functionalization of the surface can be reached for these MNPs. Along these lines, polymers (mainly polystyrene and polypropylamine) and dendrimers have been successfully used in the past as multivalent spacers to increase loadings of catalysts, adsorbents

- 
- [a] E. Folgado, Dr M. Guerre, Dr V. Ladmiral, Dr B. Améduri, Dr A. Ouali (s)  
Institut Charles Gerhardt – UMR 5253 – CNRS, UM, ENSCM; 8 Rue de l'Ecole Normale, F-34296 Montpellier Cedex 5  
E-mail: armelle.ouali@enscm.fr
- [b] N. Mimouni, V. Collière, Dr C. Bijani, Dr K. Moineau-Chane Ching, Dr A.-M. Caminade  
Laboratoire de Chimie de Coordination du CNRS, 205 Route de Narbonne, BP 44099, F-31077 Toulouse
- [c] LCC-CNRS, Université de Toulouse, CNRS, Toulouse, France.

Supporting information for this article is given via a link at the end of the document. ((Please delete this text if not appropriate))

or dyes on the surface of such MNPs.<sup>[7,8,9b,12]</sup> Dendrimers are synthesized by a step-by-step method which affords perfect control of their size and structure, as well as the incorporation of a great number of functions.<sup>[2]</sup> In this project, they were thus preferred as multivalent spacers between the surface of the MNP and the PVDF chain to reach a fine-tuning of the number of polymer chains grafted. Among the possible dendritic spacers available, the zeroth generation of phosphorous dendrimers was chosen because it was previously shown to allow a significant loading enhancement in the case of Pd catalysts.<sup>[9b]</sup>

Therefore, this article reports the preparation and characterization of new dissymmetric dendrimers bearing ten PVDF branches and one flexible arm ended by a pyrene moiety able to interact with the graphene surface (Figure 1). The association of these dendrimers with MNPs was studied by fluorescence spectroscopy, and the thermal stability of these interactions was also evaluated. Hybrids MNPs were prepared and characterized by High-Resolution Transmission Electron Microscopy (HRTEM) and comparative elemental analysis with naked MNPs to evaluate the loading of dendritic PVDF.

## Results and Discussion

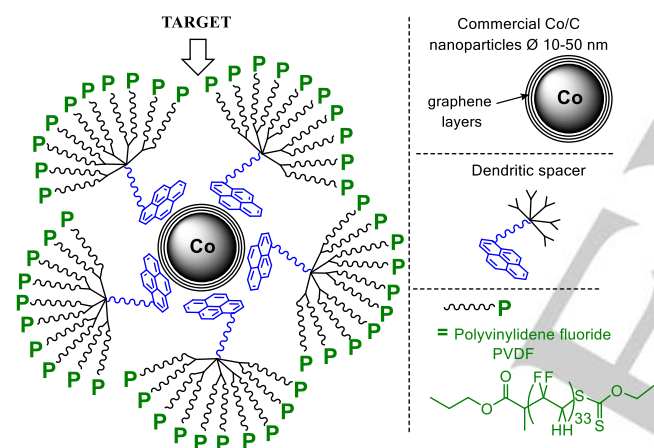
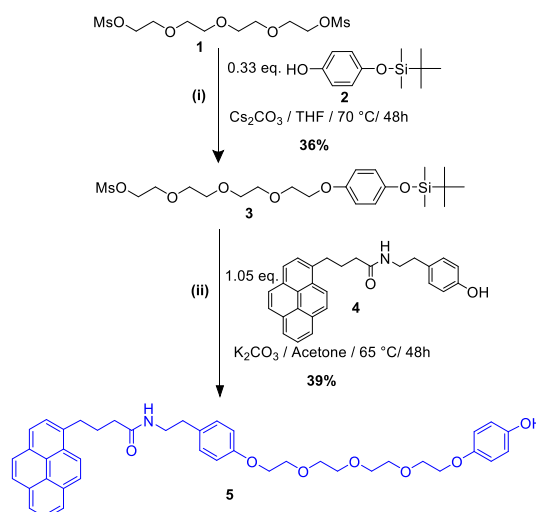


**Figure 1.** Targeted multifunctional materials: study of the non-covalent coating of Co/C magnetic nanoparticles (MNPs) by pyrene-tagged PVDF-dendrons.

Pyrene tagged spacer **5** (Scheme 1), consisting in a tetraethylene glycol moiety bearing one pyrene tag at one chain end and a phenol function at the other end, was prepared in two steps from the corresponding tetraethylene glycol dimesylate **1** (see SI, S2). The first step (Scheme 1 (i)) consisted in the substitution of one of the mesylate groups of **1** with 4-([tert-butyl(dimethyl)silyl]oxy)phenol **2**. The second step (Scheme 1 (ii)) involved the nucleophilic substitution of pyrene containing phenol **4** onto the remaining mesylate of compound **3** in the presence of a base ( $K_2CO_3$ ) in refluxing acetone. To our delight, under these reaction conditions, the deprotection of the protecting trialkylsilyl group ( $SiMe_2tBu$ ) also occurred. Due to this simultaneous substitution and deprotection, the synthesis of **5** from **3** was possible in one step. Afterward, a nucleophilic substitution reaction allowed the coupling of spacer **5** containing the pyrene moiety with unsymmetrical core **6** prepared

according to previously reported methods<sup>[13]</sup> (Scheme 2 (i)). The reaction was monitored by  $^{31}P$ -NMR spectroscopy by following the disappearance of the initial signals at 20.72 ppm. Compound **7** was obtained in good yield (71%) after purification by flash chromatography and characterized by  $^1H$ ,  $^{31}P$ , and  $^{13}C$  NMR. The  $^{31}P$ - $\{^1H\}$  NMR spectrum obtained was relatively complex due to second-order effects (see SI, Figure S5.5). The grafting of the flexible pyrene-tagged arm was indeed found to induce a slightly different environment for the two phosphorus atoms bearing the same substituents (two  $-O-C_6H_4-CHO$  groups) leading to their magnetic non-equivalence (see SI, Figure S2.1). The signals were exhaustively analyzed, and an NMR signal line shape fitting analysis allowed the calculations of the chemical shifts and coupling constants of the three phosphorous atoms. This non-equivalence of the phosphorous atoms as well as the large differences between coupling constants have already been reported for hexasubstituted cyclotriphosphazenes involving five identical substituents.<sup>[14]</sup> Hence, the condensation of the aldehyde functions of **7** with dichlorothiophosphorhydrazide **8** yielded compound **9** bearing five new phosphorous atoms as divergence points in high yield (90%). Besides the complex signals corresponding to the core (Figure S5.8), the  $^{31}P$  NMR spectrum of compound **9** displays three signals in a 2/1/2 ratio, corresponding to the five  $P(S)Cl_2$  functions (Figure S5.9). The small signal can be assigned to the  $P(S)Cl_2$  group linked to the phosphorus of  $N_3P_3$  that bears the pyrene, whereas one of the other signals corresponds to two  $P(S)Cl_2$  functions on the same side as the pyrene, while the other to the two  $P(S)Cl_2$  functions on the opposite side, relative to the  $N_3P_3$  plane. Such an observation has already been reported.<sup>[15]</sup> Next, the growth of dendron **9** was achieved by performing nucleophilic substitution of the ten terminal chlorine atoms ( $P(S)Cl_2$  functions) by phenol **10** using previously reported experimental conditions.<sup>[4]</sup> Peripheral acetylenic functions of dendron **11** were then allowed to react with azide-functionalized PVDF<sup>[4,16]</sup> **12** to lead to the targeted dendron **13** (yield 95%) possessing a pyrene core and 10 PVDF chains.

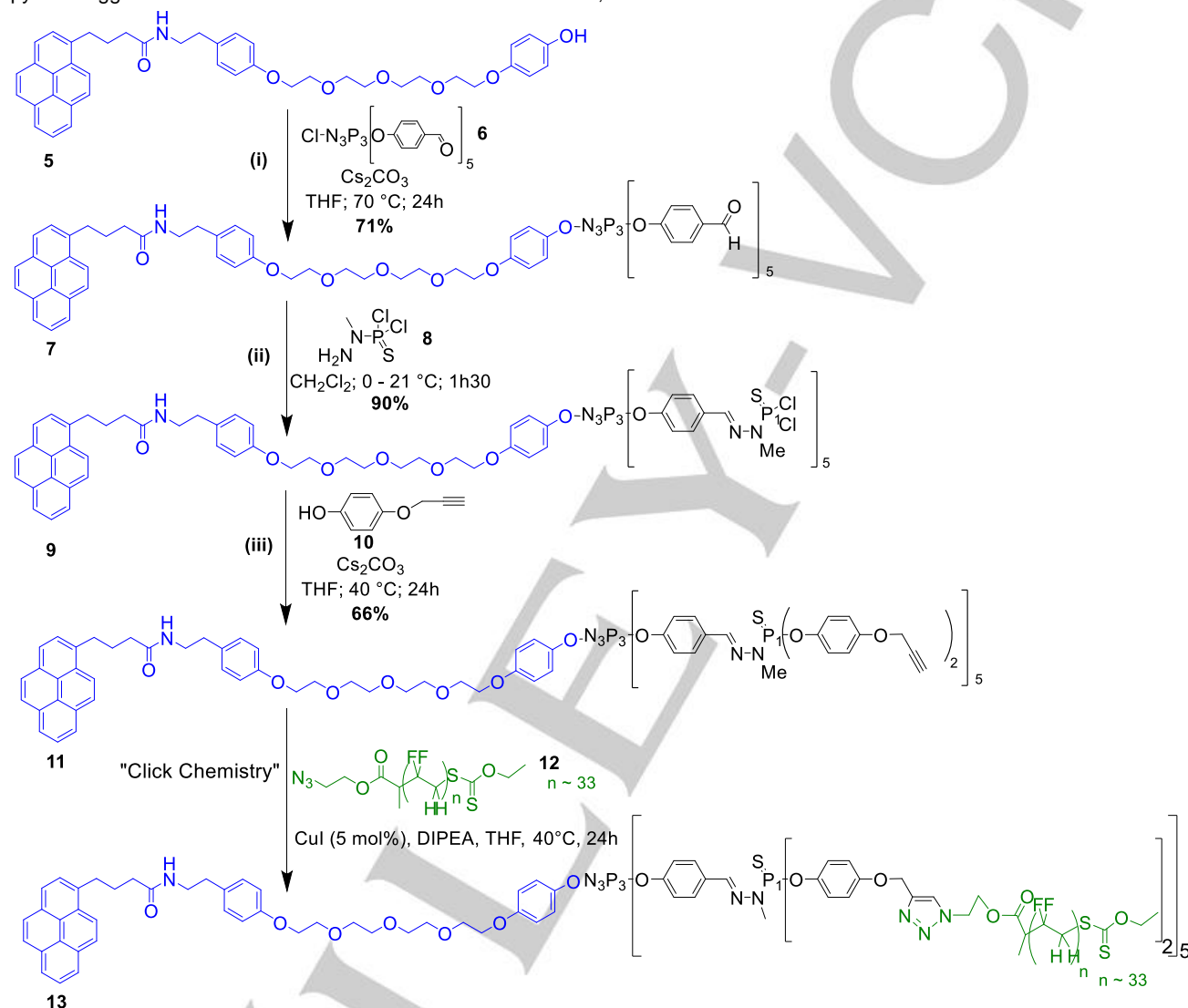


**Scheme 1.** Preparation of the pyrene-tagged arm to be linked to the dendritic core

The reaction was monitored by FT-IR spectroscopy (disappearance of the characteristic frequency of the azido group of **12** at  $2111\text{ cm}^{-1}$ ) and  $^1\text{H}$ , and  $^{31}\text{P}$  NMR spectra confirmed the completion of the reaction. It is worth noting that the structures of compounds **9** and **11** were confirmed by matrix-assisted laser desorption/ionization coupled time-of-flight mass spectroscopy (MALDI-TOF) (see SI, Figures S5.11 and S5.15, resp.).

To gain further insights into the interactions existing between the pyrene-tagged dendrimers and the surface of the MNPs,

fluorescence spectrometry was employed. This technique can quantify the amounts of pyrene moieties present in solution. Monomer emission of pyrene occurs within  $370\text{-}390\text{ nm}$  whereas that of the excimer is observed within  $465\text{-}500\text{ nm}$ .<sup>[10]</sup> An excimer is a bimolecular complex where one molecule exists in an excited state while the other one is in the ground state. When two pyrene molecules are in close proximity, they form an excimer that fluoresces prominently at a longer wavelength compared to monomeric pyrene (Figure 2).



**Scheme 2.** Attachment of the pyrene-tagged arm to the dendritic cyclotriphosphazene core, dendritic growth, and grafting of the PVDF chains on the dendrimer surface (DIPEA = *N,N*-diisopropylethylamine).

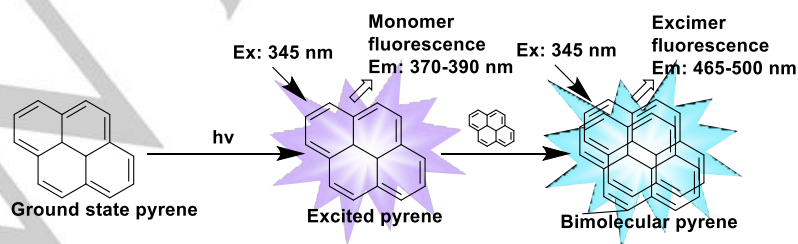


**Figure 2.** Pyrene Excimer formation, Ex: Excitation, Em: Emission Monomer Em. of pyrene within 370-390 nm. Excimer emission within 465-500 nm

To assess the existence of interactions between the graphene surface and the pyrene moiety, the methodology previously reported to get insight into the  $\pi$ -stacking interactions between pyrene-tagged polymers, and carbon nanotubes was employed.<sup>[10]</sup> A preliminary UV spectroscopy study allowed the determination of the wavelength of maximum absorption ( $\lambda_{\text{max}}$ ) for **11** and **13** (340 nm and 320 nm, respectively, for solutions at  $9.25 \times 10^{-6} \text{ mol L}^{-1}$  of each compound in THF/water (2:5 vol/vol) for an absorbance below 0.1 a.u.). Afterward, the emission spectra of both compounds were recorded by irradiation at their respective  $\lambda_{\text{max}}$  (340 nm for **11** and 320 nm for **13**). A THF/water (2:5) mixture was chosen for these studies since it was demonstrated to be optimal to achieve  $\pi$ -stacking of phosphorous pyrene-tagged dendrons decorated with related aldehyde and phosphine moieties onto Co/C MNPs.<sup>[9b]</sup> Less polar solvents (e. g. THF/water mixtures with THF/water > 2:5) were indeed shown to disfavor  $\pi$ -stacking interactions while more polar solvents did not sufficiently solubilize the pyrene-tagged organic molecules.

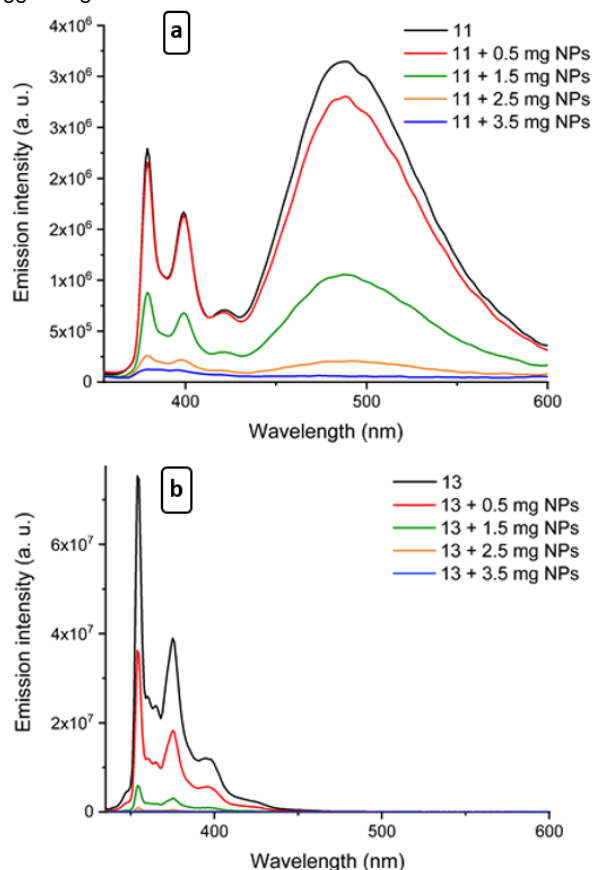


**Figure 3.** Fluorescence emission spectra of pyrene-acetylenic dendrimer **11** (a) and pyrene-PVDF dendrimer **13** (b) in the absence of Co/C-MNPs in THF/water (2:5) (black curve). After each addition of MNPs, the suspension was sonicated, then magnetically decanted with a magnet and the emission spectra of the supernatant were recorded and reported in these graphics (see detailed conditions in SI S3)

The emission spectra of dendrimers **11** and **13** displayed three sharp bands around 350-450 nm assigned to the pyrene monomer. Only compound **11** exhibited one extra broadband at 460 nm corresponding to the excimer emission (Figure 3, black line). It is worth noting that the formation of excimers is not visible in the case of PVDF-functionalized molecule **13**. This observation might be rationalized by the steric hindrance induced by the PVDF chains in compound **13** preventing interactions between two pyrene units. Aliquots of Co/C MNPs were then successively added to these homogeneous solutions (Figures 3, Experimental section and SI S3). After each addition, the suspension was sonicated for 30 min, the MNPs removed by magnetic decantation and the supernatant analyzed by fluorescence spectroscopy. Each addition was found to induce a decrease of the emission intensity (Figure 3 a,b). The observed extinction of the emission corresponded to a decrease of the concentration of pyrene-tagged dendrimers **11** or **13** in the supernatant. This strongly suggested that **11** and **13** interacted with the MNPs (Figure 3 a,b). These results thus support the existence of interactions between the graphene surface of the MNPs and the pyrene moieties of dendrimers **11** and **13**.

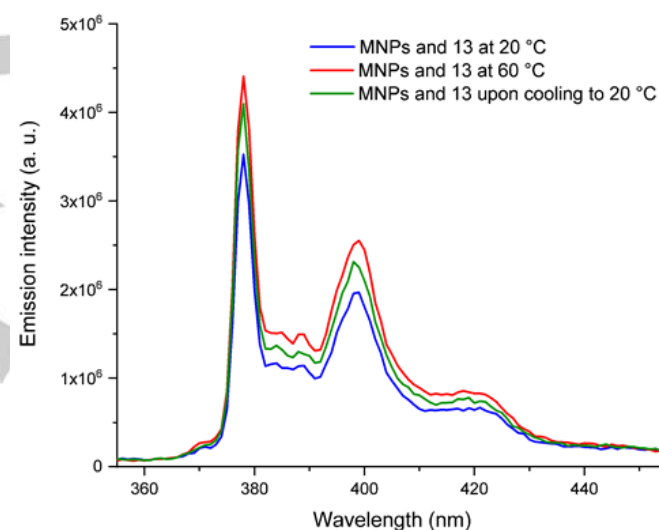


**Figure 4:** Reversibility test: a suspension of **13** and MNPs was sonicated for 30 minutes at 20 °C, magnetically decanted and the fluorescence spectrum of the supernatant recorded (blue curve). The mixture (supernatant and MNPs) was then heated to 60 °C for 10 h, and the spectrum of the resulting supernatant analyzed (red curve). Upon cooling to 20 °C, the concentration of **13** in the solution decreased (green curve). (see details in Experimental section and SI)

Next, the reversibility of the  $\pi$ -stacking interactions was evaluated. Indeed, as previously reported, the efficiency of the interactions between the pyrene moiety and the graphene surface may depend on the temperature.<sup>[9]</sup>  $\pi$ -stacking interactions were found to be inefficient at temperatures exceeding 60 °C but to be reversible since the  $\pi$ -stacking



interactions were restored upon cooling. For this study, pyrene-tagged dendrimer **13** was used.

Therefore, a suspension of **13** and MNPs was sonicated for 30 minutes at 20 °C first, then magnetically decanted with a magnet and the fluorescence spectrum of the supernatant further recorded (Figure 4, blue curve). The mixture (supernatant and MNPs) was then heated up to 60 °C for 10 h, and the spectrum of the resulting supernatant analyzed (Figure 4, red curve). The latter experiment indicated that the concentration of pyrene-tagged dendritic PVDF **13** significantly increased in accordance with a partial release of **13** from the surface of the MNPs at 60 °C. Upon cooling to 20 °C, the concentration of **13** in the solution decreased (Figure 4, green curve) suggesting partial reversibility of the  $\pi$ -stacking interactions. Importantly, the fluorescence spectra recorded after 1h or 12h after return to ambient temperature were identical. Contrary to pyrene-tagged dendritic phosphines previously reported,<sup>[9b]</sup> the reversibility is not complete.

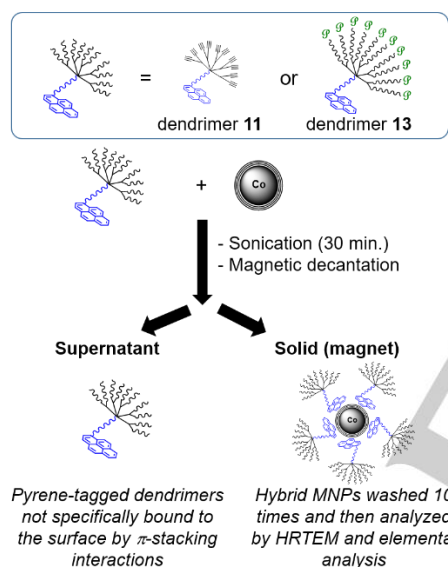


**Figure 5.** The procedure used for the preparation of hybrid NPs composed of Co/C MNPs coated with pyrene-tagged dendrimers **11** or **13** (dendrimers are used in large excess compared to dendrimers-to-MNPs ratios used for fluorescence studies, see SI, S3).

After having studied the interactions of pyrene-tagged dendrimers **11** and **13** with the graphene surface of MNPs by fluorescence spectroscopy and assessed the existence and partial reversibility (case of **13**) of  $\pi$ -stacking interactions, preliminary tests for the preparation of hybrid MNPs were performed according to the protocol depicted in Figure 5: (i) a homogeneous suspension of pyrene-tagged dendrimers **11** or **13** in large excess and MNPs in a THF/water (2:5) solution was prepared and sonicated for 30 min; (ii) the nanoparticles were then magnetically decanted and rinsed ten times with hot THF/water mixtures to remove ungrafted pyrene-tagged dendrimers **11** or **13** from the medium; (iii) the MNPs were recovered using a magnet, then dried and analyzed by HRTEM to evaluate the grafting of the MNPs with PVDF, and by

elemental analysis to determine the amount of polymers incorporated in these hybrid constructs. To optimize the grafting process and according to previously reported protocols,<sup>[9b]</sup> dendrimers, **11** or **13** were introduced in large excess in these experiments (dendrimer/MNPs ratio roughly 90 times higher than those used for fluorescence studies, see S3 in SI). The excess of pyrene-tagged dendrimers not specifically bound through  $\pi$ -stacking interactions to the graphene surface was expected to be removed by washing.<sup>[9b]</sup> TEM images showed the presence of MNPs surrounded by pyrene-tagged dendrons **11** (Figure 6a) or **13** (Figure 6b). EDX analyses confirmed the presence of Co in the dark areas, while the lighter grey shells around the Co core mainly displayed the presence of heteroelements in high amount (for dendrimer **11**: P and S, characteristic elements of dendritic skeleton; for dendrimer **13**: P, S and F, characteristic elements of PVDF chains and dendritic spacers, see SI, Fig. S4).

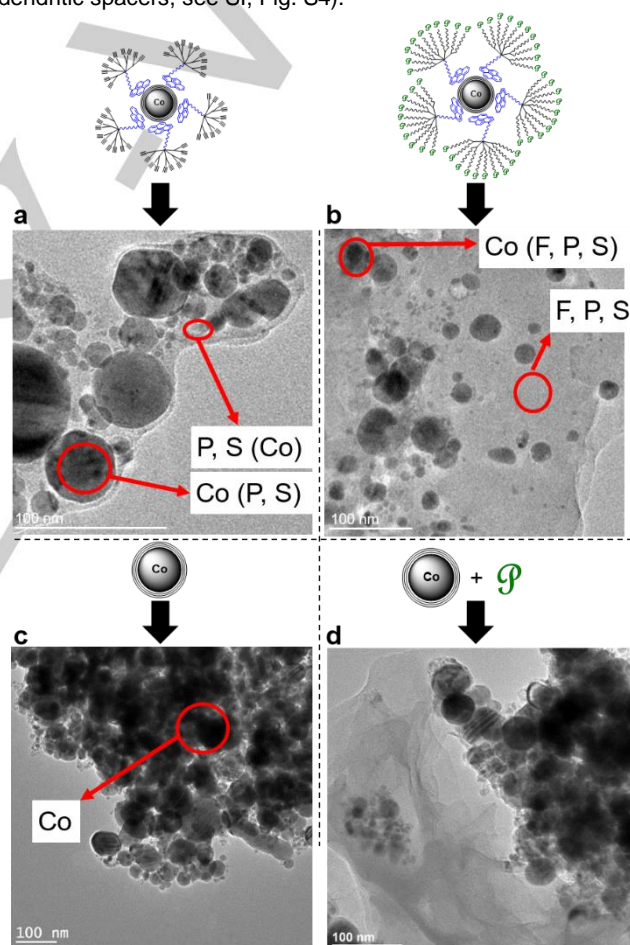


**Figure 6:** HRTEM images of a) MNPs grafted with acetylenic dendrimer **11**. b) MNPs grafted with dendritic PVDF **13**. c) naked Co/C MNPs. d) attempts of grafting using MNPs and PVDF without pyrene unit. In cases, a, b and d, the procedure detailed in Figure 5 was employed.

It is, however, worth noting that Figure 6b shows the presence of large areas containing only dendritic PVDF (light grey areas on the images) sometimes reaching several tens of nanometers in size. This suggests that the washing procedure used to remove

ungrafted dendritic PVDF **13** was not completely efficient. The high crystallinity and poor solubility of PVDF is likely responsible for the incomplete removal of dendritic PVDF **13** in excess and additional washing steps with solvents including DMF, and fluorinated solvents did not improve the results. The magnetic decantation did not isolate only the functionalized MNPs, but it also trapped non-negligible amounts of free (not bound to the MNPs by  $\pi$ -stacking) dendritic PVDF **13**. Interestingly, when performing the procedure depicted in Figure 5 using **11** instead of **13**, the pyrene-tagged dendrimers in excess that were not specifically associated with MNPs through  $\pi$ -stacking interactions were efficiently removed. Therefore, the resulting MNPs were found to be surrounded by thin light grey shells containing the phosphorous dendrons **11** according to EDX experiments (Figure 6a). The significantly lower efficiency of the washing procedures in the case of dendrimer **13** was confirmed by elemental analysis which showed that up to 7 mmol of pyrene-tagged dendrons were associated with one gram of MNPs. Such a loading is much higher than (and therefore not consistent with) those calculated for pyrene-tagged dendrimer **11** (0.04 mmol of pyrene tag per gram of MNPs) and those previously reported for pyrene-tagged dendritic phosphines (0.03 mmol of pyrene tag per gram of MNPs).<sup>[7]</sup> Interestingly, compared to the “naked” Co/C MNPs (Figure 6c), the MNPs functionalized by pyrene-tagged dendrimers (Figure 6a and b) were found to be less aggregated. In addition, when non-functional PVDF chains (i.e., not bearing pyrene moieties) were used, a complete segregation between dendritic PVDF and the MNPs was observed (Figure 6d). This result was consistent with fluorescence studies and highlighted the crucial role of the pyrene moiety in the grafting process.

## Conclusions

The objective of this work was to study the non-covalent coating of MNPs with pyrene-tagged poly(vinylidene fluoride). Phosphorous dendrimers bearing a pyrene moiety were selected as spacers between the surface of the MNP and the polymer chains. Indeed, the pyrene unit was expected to interact with the graphene surface. The dendritic spacer decorated with acetylenic functions was successfully prepared and fully characterized (compound **11**). Azido-functionalized PVDF chains were next successfully grafted onto each branch of dendrimer **11** by using Huisgen [3+2] cycloadditions (“click chemistry”). Afterwards, the association of pyrene-tagged dendrimers **11** and **13** (decorated with PVDF chains) with commercially available Co/C MNPs was studied. Fluorescence studies confirmed the existence of interactions between pyrene-tagged dendrimers and the MNPs as well as the crucial role played by the pyrene moiety. Moreover, dendritic PVDF **13** was found to be released upon temperature increase and interestingly, the partial reversibility of the  $\pi$ -stacking interactions between **13** and the graphene-functionalized surface of the MNPs was observed upon temperature decrease. Afterward, the syntheses of hybrid MNPs obtained from pyrene-tagged dendrimers **11** and **13** were

achieved according to previously reported protocols (i. sonication of a mixture of MNPs and pyrene-tagged dendrimers; ii. magnetic decantation. iii. washings of the resulting hybrid MNPs). The hybrid MNPs syntheses were performed in the presence of large excess of pyrene-tagged dendrimers to optimize the grafting process and the excess of pyrene-tagged dendrimers not specifically bound through  $\pi$ -stacking interactions to the graphene surface can be removed by washing. TEM images and related EDX experiments revealed in both cases the presence of pyrene-tagged dendrimers surrounding the MNPs. On the contrary and interestingly, complete phase segregation occurred when associating “naked Co/C MNPs” and pyrene-free PVDF which highlighted the crucial role of the pyrene moiety in the grafting process and was thus consistent with fluorescence studies. As expected, in the case of **11**, thin shells containing the characteristic P and S heteroatoms were observed. For **13**, the organic shells containing P, S and F atoms were found to be larger (up to several tens of nm). This showed that some free dendritic PVDF **13** was also trapped despite careful washing in contrast to the case of the more soluble and less crystalline compound **11** which excess could be completely removed by washings. These MNP-dendrimer constructs were also shown by fluorescence studies to display a thermo-responsive behavior whereby the non-covalent interactions (and thus the grafting) were partially reversible upon heating. This interesting property might allow the future use of such hybrid MNPs in thermo-responsive materials combining magnetic properties together with the well-known and outstanding features of PVDF for high-tech applications. More generally, the first coating of MNPs with polymers through  $\pi$ -stacking interactions reported here opens the way to more modular and tunable nanocomposites.

## Experimental Section

The preparation and characterization (including NMR and mass spectra) of compounds **3**, **5**, **7**, **9**, **11** and **13** are detailed in the Electronic Supporting Information. The  $\pi$ -stacking procedures are summarized below (for more details and EDX spectra, see Supporting Information section).

### Fluorescence studies with **11** and **13** (Figure 3)

Solutions of dendrimers **11** or **13** ( $9.25 \times 10^{-6}$  mol L<sup>-1</sup> in a THF-water (2:5)) were prepared and their fluorescence recorded. Aliquots of Co/C MNPs were then successively added to these homogeneous solutions (0.5 mg for the first addition and 1 mg for each further addition, Figure 3). After each addition, the suspension was sonicated for 30 min, the MNPs removed by magnetic decantation and the supernatant analyzed by fluorescence spectroscopy.

### Fluorescence studies to perform reversibility test with **13** (Figure 4)

A suspension of **13** (solution in a THF-water (2:5);  $9.25 \times 10^{-6}$  mol.L<sup>-1</sup>) and MNPs was sonicated for 30 minutes at 20 °C, magnetically decanted with a magnet and the fluorescence spectrum of the supernatant recorded (blue curve). The mixture (supernatant and MNPs) was then heated to 60 °C for 10 h, and the spectrum of the resulting supernatant analyzed

(red curve). Upon cooling to 20 °C, the concentration of 13 in the solution decreased (green curve). Importantly, the fluorescence spectra recorded after 1 hour or 12 hours after return to ambient temperature were found to be identical.

### Grafting measurements with 13

A mixture of THF-water 2:5 (15 mL) was added to Co/C nanoparticles (15 mg) and pyrene-tagged dendrimer **13** (194 mg,  $7.10^{-3}$  mmol) and were sonicated for 30 minutes at 20 °C. The nanoparticles were then magnetically decanted and rinsed ten times with the same hot solvent mixture (THF-water 2:5) to try to remove ungrafted pyrene-tagged dendrimer from the medium. The recovered MNPs were dried and analyzed by TEM (see Figure 6b) and by elemental analysis. By comparison with the result obtained for free nanoparticles, the loading of the pyrene-tag was calculated.

### Acknowledgments

The authors thank Arkema S. A. (Pierre Bénite, France) for providing VDF and the Ministère de l'Éducation Nationale et de l'Enseignement Supérieur et de la Recherche for Marc Guerre's PhD grant.

**Keywords:** dendrimer • magnetic nanoparticles •  $\pi$ -stacking • poly(vinylidene fluoride) • pyrene

- [1] For some reviews, see: (a) J. Gonzalez-Benito, D. Olmos, *Society of Plastics Engineers*, **2010**, *31*, 946-955; (b) M. Supova, G. S. Martynkova, K. Barabaszova, *Sci. Adv. Mater.* **2011**, *3*, 1-25; (c) G. D. Smith, D. Bedrov, *Langmuir* **2009**, *25*, 11239-11243; (d) P. Ajayan, L. S. Schadler, P. V. Braun, *Nanocomposite Science and Technology*; Wiley-VCH: Weinheim, **2003**; (e) P. Gomez-Romero, C. Sanchez, *Functional Hybrid Materials*; Wiley-VCH: Weinheim, **2004**; (f) H. Zou, S. Wu, J. Shen, *Chem. Rev.* **2008**, *108*, 3893-3957; (g) C. M. Lukehart, R. A. Scott, *Nanomaterials: Inorganic and Bioinorganic Perspectives*; Wiley: New York, **2008**; (h) S. D. Achilleos, M. Vamvakaki, *Materials*, **2010**, *3*, 1981-2026; (i) M. Krishnamoorthy, S. Hakobyan, M. Ramstedt, J. E. Gautrot, *Chem. Rev.* **2014**, *114* (21), 10976-11026; (j) S. Xia, L. Song, V. Körstgens, M. Opel, M. Schwartzkopf, S. V. Roth, P. Müller-Buschbaum, *Nanoscale* **2018**, *25*, 11930-11941; (k) D. Kim, K. Shin, S. G. Kwon, T. Hyeon, *Adv. Mater.* **2018**, 1802309.
- [2] Dendrimers are perfectly defined globular macromolecules with a regular hyperbranched structure and tunable multivalent surfaces. They find applications in many scientific fields including catalysis, nanomedicine and material science. For some examples: (a) D. A. Tomalia, J. B. Christensen, U. Boas, *Dendrimers, Dendrons, and Dendritic Polymers*; Cambridge University Press: New York, **2012**; (b) A. M. Caminade, C. O. Turrin, R. Laurent, A. Ouali, B. Delavaux-Nicot, *Dendrimers. Towards Catalytic, Material, and Biomedical Uses*; Wiley & Sons Ltd: Chichester, **2011**; (c) F. Vögtle, G. Richardt, N. Werner, *Dendrimer Chemistry*. Wiley VCH: Weinheim, **2009**; (d) D. Astruc, E. Boisselier, C. Ornelas, *Chem. Rev.* **2010**, *110*, 1857-1959.
- [3] (a) B. Ameduri, *Chem. Rev.* **2009**, *109*, 6632-6686; (b) J. S. Humphrey, R. Amin-Sanayei, *Vinylidene Fluoride Polymers*. Encyclopedia of Polymer Science and Technology, 3rd ed.; H. F. Mark, Ed.; Wiley: New York, **2004**; Vol. 4, pp 510-533. For original properties of PVDF-based nanocomposites, see also for recent examples: (c) Z. Li, L. Zhang, R. Qi, F. Xie, S. Qi, *J. Applied Polym. Sci.* **2016**, *133*, 43554; (d) K. Ke, P. Pötschke, N. Wiegand, B. Krause, B. Voit, *ACS Appl. Mater. Interfaces* **2016**, *8*, 14190-14199; (e) J. T. Goldbach, R. Amin-Sanayei, W. He, J. Henry, W. Kosar, A. Lefebvre, G. O'Brien, D. Vaessen, K. Wood and S. Zerafati, *Commercial synthesis and applications of poly(vinylidene fluoride)*, in *Fluorinated Polymers Vol. 2: Applications*, Chapter 6, pp 126-157, ed. B. Ameduri and H. Sawada, Royal Society of Chemistry, Cambridge, **2016**.
- [4] Noteworthy, some of us recently reported the preparation of PVDF-decorated dendrimers constituting promising candidates for applications in coatings, as processing aids or as additives for nanocomposites. E. Folgado, M. Guerre, C. Bijani, V. Ladmiraal, A.-M. Caminade, B. Ameduri, A. Ouali, *Polym. Chem.* **2016**, *7*, 6632-6686.
- [5] R. N. Grass, E. K. Athanassiou, W. J. Stark, *Angew. Chem. Int. Ed.* **2007**, *46*, 4909-4912.
- [6] Purchased from Aldrich. CAS 7440-48-4. Reference 697745.
- [7] Q.M. Kainz, O. Reiser, *Acc. Chem. Res.* **2014**, *47*, 667-677.
- [8] Q. M. Kainz, A. Schätz, A. Zöpfl, W. J. Stark, O. Reiser, *Chem. Mater.* **2011**, *23*, 3606-3613.
- [9] a) S. Wittmann, A. Schätz, R. N. Grass, W. J. Wendelin *Angew. Chem. Int. Ed.* **2010**, *49*, 1867-1870; b) M. Keller, V. Collière, O. Reiser, A. M. Caminade, J. P. Majoral, A. Ouali, *Angew. Chem. Int. Ed.* **2013**, *52*, 3626-3629.
- [10] Z. Guo, H. Yin, Y. Feng, S. He, *RSC Adv.* **2016**, *6*, 37953-37964.
- [11] In some examples, polymers are physisorbed onto the Fe/C or Co/C NPMs and these materials were shown to be less stable (leaching of MNPs). e. g. Fuhrer, R.; Schumacher, C. M.; Zeltner, M.; Stark, W. J. *Adv. Funct. Mater.* **2013**, *23*, 3845-3849.
- [12] a) C. J. Hofer, V. Zlateski, P. R. Stoessel, D. Paunescu, E. M. Schneider, R. N. Grass, M. Zeltner, W. J. Stark, *Chem. Commun.* **2015**, *51*, 1826; b) M. Zeltner, A. Schätz, M. L. Hefti, W. J. Stark, *J. Mater. Chem.* **2011**, *21*, 299; c) M. Zeltner, R. N. Grass, A. Schaetz, S. B. Bubenhofer, N. A. Luechinger, W. J. Stark, *J. Mater. Chem.* **2012**, *22*, 12064-12071; d) R. Fuhrer, E. K. Athanassiou, N. A. Luechinger, W. J. Stark, *Small*, **2009**, *5*, 383; e) X. Zhang, O. Alloul, J. Zhu, Q. He, Z. Luo, H. A. Colorado, N. Haldolaarachchige, D. P. Young, T. D. Shen, S. Wei, Z. Guo, *RSC Adv.* **2013**, *3*, 9453; f) M. Keller, A. Perrier, R. Linhardt, L. Travers, S. Wittmann, A. M. Caminade, J. P. Majoral, O. Reiser, A. Ouali, *Adv. Synth. Catal.* **2013**, *355*, 1748-1754.
- [13] (a) G. Franc G., S. Mazères, C.-O. Turrin, L. Vendier, C. Duhayon, A.-M. Caminade, J.-P. Majoral, *J. Org. Chem.* **2007**, *72*, 8707-8715; (b) O. Rolland, L. Griffe, M. Poupot, A. Maraval, A. Ouali, Y. Coppel, J.-J. Fournié, G. Bacquet, C.-O. Turrin, A.-M. Caminade, J.-P. Majoral, R. Poupot, *Chem. Eur. J.* **2008**, *14*, 4836-4850.
- [14] V. Vicente, A. Fruchier, H.-J. Cristau, *Magn. Reson. Chem.* **2003**, *41*, 183-192.
- [15] D. Riegert, A. Pla-Quintana, S. Fuchs, R. Laurent, C.O. Turrin, C. Duhayon, J.P. Majoral, A. Chaumonnot, A.M. Caminade, *Eur. J. Org. Chem.* **2013**, 5414-5422.
- [16] Copper-catalyzed azide-alkyne [3 + 2]-cycloaddition (CuAAC)CuAAC is an attractive ligation method in terms of atom-economy, high yield, reaction rate and also for the robustness of the triazole ring it generates. It has been widely exploited to design and prepare functional dendritic and polymeric architectures, including fluorinated ones. For reviews, see: (a) M. Arsenaull, C. Wafer, J.-F. Morin, *Molecules* **2015**, *20*, 9263-9294; (b) W. Xi, T. F. Scott, C. J. Kloxin, C. N. Bowman, *Adv. Funct. Mater.*, **2014**, *24*, 2572-2590; (c) J. A. Johnson, M. G. Finn, J. T. Koberstein, N. J. Turro, *Macromol. Rapid. Commun.*, **2008**, *29*, 1052-1072. For some examples: (d) S. A. McNelles, A. Adronov, *Macromolecules* **2017**, *50*, 7993-8001; (e) G. Tillet, G. Lopez, M.-H. Hung, B. Ameduri, *J. Polym. Science Part A* **2015**, *53*, 1171-1173; (f) D. Lu, M. D. Hossain, Z. Jia, M. J. Monteiro, *Macromolecules* **2015**, *48*, 1688-1702; (g) X. Feng, D. Taton, E. Ibarboure, E. L. Chaikof, Y. Gnanou, *J. Am. Chem. Soc.* **2014**, *130*, 11662-11676; (h) F. Yao, L.-Q. Xu, G.-D. Fu, B.-P. Lin, *Polym. Int.* **2012**, *61*, 749-759; (i) G. Tillet, P. De Leonardis, A. Alaeddine, M. Umeda, S. Mori, N. Shibata, S. M. Aly, D. Fortin, P. D. Harvey, B. Ameduri, *Macromol. Chem. Phys.* **2012**, *213*, 1559-1568; (j) A. Soules, B. Ameduri, B. Boutevin, G. Callega,



Macromolecules, **2010**, *43*, 4489-4499; (k) A. Carlmark, C. J. Hawker, H. Anders, M. Malkoch, *Chem. Soc. Rev.*, **2009**, *38*, 352-362; (l) V. Ladmiral, G. Mantovani, G. J. Clarkson, S. Cauet, J. L. Irwin, D. M. Haddleton, *J. Am. Chem. Soc.* **2006**, *128*, 4823-4830; (m) E. Arnaiz, E. Vacas-Cordoba, M. Galan, M. Pion, R. Gomez, MA Angeles Munoz-Fernandez, J. Javier de la Mata., *J. Polym. Science, Part A.* **2014**, *52*, 1099-1112.

WILEY-VCH

WILEY-VCH

---